Nematic order director fluctuations and nuclear magnetic relaxation of a confined liquid crystal

P. Ziherl,[1] M. Vilfan,[2] and S. Žumer[1]
[1]*Department of Physics, University of Ljubljana, Jadranska 19, 61 111 Ljubljana, Slovenia*
[2]*J. Stefan Institute, University of Ljubljana,k Jamova 39, 61 111 Ljubljana, Slovenia*
(Received 27 October 1994; revised manuscript received 11 April 1995)

The dynamics of order director fluctuations of a nematic liquid crystal confined to microcavities is studied within the Frank elastic theory. For cylindrical capillary and rectangular model cavities, constrained in one, two, and three spatial dimensions, mutually perpendicular components of fluctuations are expanded in terms of eigenfunctions of the Landau-Khalatnikov type relaxation equation. The calculated dispersion of the director fluctuations' spin-lattice relaxation rates exhibits weak dependence on the nematic structure and the confining geometry, unless the size of the cavity is close to the critical value at which the structural transition is expected. In the latter case, the low-frequency behavior of the relaxation rate is dominated by the slowest fluctuations' modes. On the other hand, the angular dependence of the relaxation rate is sensitive to details of the nematic structure in the cavity in the whole frequency range.

PACS number(s): 61.30.Cz, 76.90.+d

I. INTRODUCTION

It has been known for over 25 years that order director fluctuations are an important mechanism of nuclear magnetic relaxation in nematic liquid crystals. In 1969, Pincus [1] derived the well known dispersion relation between the spin-lattice relaxation rate T_1^{-1} and Larmor frequency ν, $T_1^{-1} \propto \nu^{-1/2}$, which was confirmed by numerous measurements [2–6]. Introducing various types of fluctuations' spectra, the original Pincus model was subsequently extended to include specific high- and low-frequency behavior [7,8]: at low frequencies the spin-lattice relaxation rate was found to be frequency independent, while at high frequencies $T_1^{-1} \propto \nu^{-2}$. In the simplest case [7] the allowed wave vectors were assumed to lie within a sphere whose radius was determined by the length of a nematic molecule to account for the high-frequency cutoff. Considering the anisotropy of the medium, the sphere was replaced by the cylinder [9,10] and by the rotational ellipsoid [11]. On the other hand, the low-frequency plateau was taken into account by leaving out the ultralong wavelength modes (which cannot exceed the size of a uniformly oriented domain) so that the integration volume in the reciprocal space was a coreless sphere [12].

In recent years, considerable attention is paid to confined liquid crystals in planar, spherical (polymer dispersed liquid crystals) [13] and cylindrical geometry (glassy capillaries, pores in Anopore and Nuclepore membranes). Nuclear magnetic resonance proved to be a useful technique when investigating structure, order, and phase transitions in both bulk [14] and confined nematic liquid crystals [15–23]. Motivated by the growing interest in microconfined liquid crystals, we studied the effect of spatial confinement on the order director fluctuations and the corresponding nuclear magnetic relaxation. The research focuses on two aspects of the topic: the behavior in the vicinity of a structural transition and the effect of the dimensionality of confinement. The confining geometries discussed in the paper are chosen in order to allow a simple analysis of the two aspects.

In particular, the collective modes of a nematic liquid crystal in a cylindrical cavity are examined; the capillary's surface is assumed to induce homeotropic molecular anchoring. In such a case the equilibrium director field configuration is described by one of the three basic structures: planar radial, planar polar, and escaped radial (Fig. 1) [24]. In this paper, only the simplest—planar radial—configuration is considered. This structure is stable in small cylinders [25], while at larger radii the escaped radial configuration is expected. The structural transition, which breaks the $C_{\infty h}$ symmetry of the planar radial structure, is expected to take place via a particular unstable eigenmode of the order director fluctuations that enables a continuous transformation of the planar configuration to the escaped one [26,27].

The influence of the dimensionality of confinement on

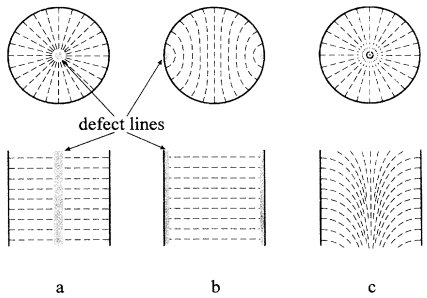

FIG. 1. Nematic structures in a capillary with strong homeotropic anchoring (top and side cross sections): planar radial (a), planar polar (b), and escaped radial (c). The defect lines are indicated by the shadowed areas; the bars denote nematic director.

order director fluctuation spin-lattice relaxation rate is studied using model systems constrained in three, two, and one spatial dimension (Fig. 2). In the first case, nematic liquid crystal is confined to a cube whose top and bottom impose homeotropic anchoring of molecules while on the other four sides planar anchoring is assumed. The ordering is therefore uniform. Next, the liquid crystal is put in an infinite waveguidelike cavity with a square cross section (which throughout the paper will be referred to as a waveguide). Again, the boundary conditions are chosen so as to induce uniform transverse orientation of the director. Finally, a nematic layer with homeotropic anchoring is considered. While the former two geometries are rather unnatural and have not been studied so far, the layer is the most common confined system.

Following the pioneering work of de Gennes and coworkers [28,29], order director fluctuations are treated within the Frank elastic theory of liquid crystals. To simplify the calculus, one elastic constant approximation is used, scalar order parameter is assumed to be spatially uniform, backflow is neglected, and the nematic-surface interaction is described by strong anchoring.

The disposition of the paper is as follows. In Sec. II the frequency-dependent part of the spectral densities constituting the order director fluctuations' spin-lattice relaxation rates is expressed as a finite sum over the fluctuations' eigenmodes and their orientation-dependent parts are calculated. Dispersion and orientational dependence of the relaxation rates are presented in Sec. III. In Sec. IV the order director fluctuation spectra in confined geometries are discussed. The results are summarized in Sec. V.

II. THEORY

The spin-lattice relaxation rate of two like spin-$\frac{1}{2}$ nuclei with constant separation distance b and gyromagnetic ratio γ is [30,14]

$$\frac{1}{T_1}=\frac{3}{2}\frac{\gamma^4\hbar^2}{b^6}\left[\frac{\mu_0}{4\pi}\right]^2[J_1(\omega)+4J_2(2\omega)] , \tag{1}$$

where ω is the circular Larmor frequency of the nuclei and $J_h(\omega)$ the spectral density of the correlation function of the orientational part of the dipolar interaction of the two spins,

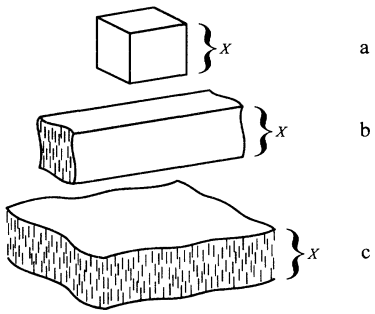

FIG. 2. The three rectangular model systems: the cube (a) is restricted in three dimensions, the waveguide (b) in two, and the layer (c) in one.

$$J_h(\omega)=\int_{-\infty}^{\infty}\langle\mathcal{F}_h(0)\mathcal{F}_h^*(t)\rangle e^{-i\omega t}dt . \tag{2}$$

The brackets denote thermal average and $\mathcal{F}_h(t)$ are time-dependent spherical harmonic functions of second order that describe the orientation of the internuclear vector with respect to the magnetic field,

$$\begin{aligned}\mathcal{F}_0(t)&=\sqrt{\tfrac{1}{8}}(1-3\cos^2\xi) ,\\ \mathcal{F}_1(t)&=\sqrt{\tfrac{3}{4}}\cos\xi\sin(\xi)e^{i\zeta} ,\\ \mathcal{F}_2(t)&=\sqrt{\tfrac{3}{16}}\sin^2(\xi)e^{2i\zeta} .\end{aligned} \tag{3}$$

$\xi=\xi(t)$ and $\zeta=\zeta(t)$ denote the polar and the azimuthal angles of the internuclear vector, which is assumed to be parallel to the long axis of the molecule.

The orientation of the internuclear vector changes due to conformational changes of the molecular structure (rotation of the functional groups) on the typical timescale of 10^{-12} s; rotation of the molecules about their long axes, where the characteristic correlation time $\sim 10^{-10}$ s; fluctuations of the molecules' long axes around the local director whose correlation time is of the order 10^{-9} s [31]; and somewhat slower thermal fluctuations of the director with correlation time of order 10^{-7} s [3]. Therefore, below ~ 1 MHz the spin-lattice relaxation rate is mainly related to order director fluctuations [3–5].

The correlation functions $\langle\mathcal{F}_h(0)\mathcal{F}_h^*(t)\rangle$ are most easily calculated when transformed from the laboratory frame with $\mathbf{e}_z\|\mathbf{B}$ to the local director's coordinate system Σ', where the z' axis coincides with the local nematic director. Following the standard procedure [32], one finds

$$\begin{aligned}\langle\mathcal{F}_0(0)\mathcal{F}_0^*(t)\rangle&=36\sin^2\psi\sin^2\theta\cos^2(\theta)\langle\mathcal{F}_1'(0)\mathcal{F}_1'^*(t)\rangle ,\\ \langle\mathcal{F}_1(0)\mathcal{F}_1^*(t)\rangle&=[\cos^2\psi\cos^2\theta+\sin^2(\psi)(2\cos^2\theta-1)^2]\langle\mathcal{F}_1'(0)\mathcal{F}_1'^*(t)\rangle ,\\ \langle\mathcal{F}_2(0)\mathcal{F}_2^*(t)\rangle&=4\sin^2(\theta)(\cos^2\psi+\sin^2\psi\cos^2\theta)\langle\mathcal{F}_1'(0)\mathcal{F}_1'^*(t)\rangle .\end{aligned} \tag{4}$$

ψ and θ (and ϕ, which does not enter the above expressions directly) are the parameters of Euler rotation, which transforms the laboratory coordinate system Σ to the reference frame Σ'. If only the lowest terms of the fluctuating director field are retained and the uniaxial symmetry of the nematic phase is taken into account,

$$\langle\mathcal{F}_1'(0)\mathcal{F}_1'^*(t)\rangle=S^2\langle\delta\mathbf{n}(0)\cdot\delta\mathbf{n}(t)\rangle , \tag{5}$$

where S is the usual scalar orientational order parameter and $\delta\mathbf{n}$ is the fluctuating component of the director in coordinate system Σ'.

Since both the director field and $\langle \mathcal{F}_1'(0)\mathcal{F}_1'^*(t)\rangle$ are generally nonuniform, the autocorrelation functions [Eq. (4)] are spatially dependent. But the diffusion of nematic molecules in the capillary is much faster than the relaxation of longitudinal magnetization. The time required for a molecule to diffuse across the capillary is $\tau \sim R^2/D$, where R is the radius of the capillary and D is the diffusion coefficient. The radii of cylindrical cavities in Anopore and Nuclepore membranes are of the order 100 nm and a typical value of D for nematic liquid crystals is 5×10^{-11} $m^2 s^{-1}$; therefore, $\tau \sim 2\times10^{-4}$ s. In the kHz range, where order director fluctuations are important, the proton spin-lattice relaxation time is of the order 10^{-2} s [3]. Since $T_1 \gg \tau$, the relaxation rate [Eq. (1)] can be spatially averaged,

$$\frac{1}{T_1} \rightarrow \overline{\frac{1}{T_1}} = \frac{1}{V}\int \frac{1}{T_1} dV \ . \tag{6}$$

Using Eqs. (2), (4), and (5) and assuming that the order parameter is spatially uniform [$S(\mathbf{r})=S$],

$$\overline{J_h}(\omega) = g_h(\alpha) S^2 \int_{-\infty}^{\infty} \overline{\langle \delta\mathbf{n}(0)\cdot\delta\mathbf{n}(t)\rangle} e^{-i\omega t} dt \ , \tag{7}$$

where

$$\begin{aligned} g_0(\alpha) &= 36\,\overline{\sin^2\psi \sin^2\theta \cos^2\theta} \ , \\ g_1(\alpha) &= \overline{\cos^2\psi \cos^2\theta + \sin^2(\psi)(2\cos^2\theta - 1)^2} \ , \\ g_2(\alpha) &= 4\,\overline{\sin^2(\theta)(\cos^2\psi + \sin^2\psi\cos^2\theta)} \ . \end{aligned} \tag{8}$$

$g_h(\alpha)$ denotes the orientation-dependent part of $\overline{\langle \mathcal{F}_h(0)\mathcal{F}_h^*(t)\rangle}$, which is a function of α, the angle between the magnetic field, and the axis of the capillary (Fig. 3).

In order to calculate the spectral density, the correlation function $\overline{\langle \delta\mathbf{n}(0)\cdot\delta\mathbf{n}(t)\rangle}$ must be determined.

A. Eigenmodes of order director fluctuations

Generally, the evolution of the nematic liquid-crystalline system depends on both velocity and director fields: the relaxation of the fluctuating director is accompanied by the hydrodynamic flow. This backflow effectively reduces the apparent viscosity, i.e., speeds up the relaxation [33]. Although it was recently shown that in the vicinity of the surface the inclusion of the fluid velocity has a more remarkable consequence than just changing the viscosity [34], a useful and common simplification of the problem is to neglect the coupling to the hydrodynamic flow, which makes the calculation much less involved.

Temporal dependence of the fluctuations is governed by the generalized Landau-Khalatnikov relaxation law [35], deduced from Leslie's equations of nematodynamics [36] upon assumption that there is no flow. In this case, the rate of change of the director is proportional to the molecular field [defined only within the Lagrange multiplier $\lambda(\mathbf{r},t)\mathbf{n}(\mathbf{r},t)$],

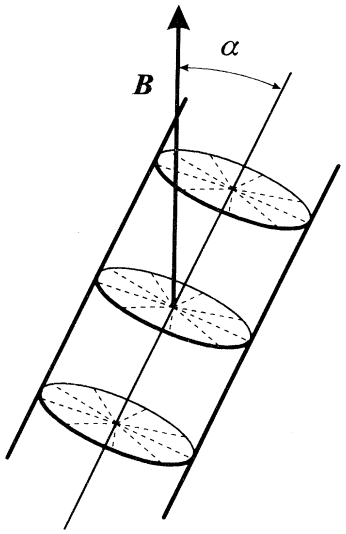

FIG. 3. Capillary with planar radial structure in the laboratory coordinate system, where the z axis is parallel to the magnetic field. The planar radial director configuration is indicated by the bars.

$$\eta \frac{\partial n_\alpha}{\partial t} = \partial_\beta \frac{\partial(\delta f)}{\partial(\partial_\beta n_\alpha)} - \frac{\partial(\delta f)}{\partial n_\alpha} + \lambda n_\alpha \ , \tag{9}$$

where $n_\alpha = n_\alpha(\mathbf{r},t)$ are the components of the nematic director, η is an effective viscosity, and δf is the elastic free energy density

$$\begin{aligned} \delta f = \tfrac{1}{2}\{ & K_{11}[\nabla\cdot\mathbf{n}]^2 + K_{22}[\mathbf{n}\cdot\nabla\times\mathbf{n}]^2 \\ & + K_{33}[\mathbf{n}\times(\nabla\times\mathbf{n})]^2\} \ , \end{aligned} \tag{10}$$

where $\mathbf{n}=\mathbf{n}(\mathbf{r},t)$ (at usual NMR frequencies the magnetic term $-(\chi a/2\mu_0)(\mathbf{n}\cdot\mathbf{B})^2$ can be omitted). Since the nematic director is a unit vector, the function $\lambda(\mathbf{r},t)$ is determined by the condition

$$\frac{\partial \mathbf{n}(\mathbf{r},t)}{\partial t} \perp \mathbf{n}(\mathbf{r},t) \ . \tag{11}$$

The analysis is considerably simplified in the one-constant approximation with $K_{11}=K_{22}=K_{33}=K$; in this case Eq. (9) is reduced to [36]

$$\eta \frac{\partial \mathbf{n}(\mathbf{r},t)}{\partial t} = K\nabla^2\mathbf{n}(\mathbf{r},t) + \lambda(\mathbf{r},t)\mathbf{n}(\mathbf{r},t) \ . \tag{12}$$

1. Cylindrical capillary

Due to thermal excitation, the nematic director fluctuates around the average configuration described by $\mathbf{n}_0=\mathbf{e}_r$. Assuming the amplitudes of the deflections are small, the fluctuating director field is given by $\mathbf{n}=\mathbf{n}_0+\delta\mathbf{n}(\mathbf{r},t)$ with

$$\delta\mathbf{n}(\mathbf{r},t) = \mathcal{P}(\mathbf{r},t)\mathbf{e}_\varphi + \mathcal{A}(\mathbf{r},t)\mathbf{e}_z \ . \tag{13}$$

The amplitude of the planar fluctuations (parallel to the unit vector $\mathbf{e}_\varphi$) is denoted by $\mathcal{P}(\mathbf{r},t)$, while $\mathcal{A}(\mathbf{r},t)$ stands for the amplitude of the axial fluctuations, where the

deflection of the director is parallel to the axis of the capillary.

According to Eq. (11), the radial component of the right-hand side of Eq. (12) should vanish, giving

$$\lambda(\mathbf{r},t)=K\left[\frac{1}{r^2}+\frac{2}{r^2}\frac{\partial\mathcal{P}(\mathbf{r},t)}{\partial\varphi}\right] . \tag{14}$$

In order to calculate the spectral density $\overline{J_h}(\omega)$, both planar and axial fluctuations have to be decomposed into eigenmodes $P(\mathbf{r},t)$ and $A(\mathbf{r},t)$ with a simple temporal dependence, which are the eigenfunctions of the relaxation equation (12). Inserting Eqs. (13) and (14) into Eq. (12) and keeping the linear terms only, one finds

$$\eta\frac{\partial P(\mathbf{r},t)}{\partial t}=K\left[\frac{\partial^2}{\partial r^2}+\frac{1}{r}\frac{\partial}{\partial r}+\frac{1}{r^2}\frac{\partial^2}{\partial\varphi^2}+\frac{\partial^2}{\partial z^2}\right]P(\mathbf{r},t) \tag{15}$$

for the planar eigenmodes and

$$\eta\frac{\partial A(\mathbf{r},t)}{\partial t}=K\left[\frac{\partial^2}{\partial r^2}+\frac{1}{r}\frac{\partial}{\partial r}+\frac{1}{r^2}\frac{\partial^2}{\partial\varphi^2}+\frac{\partial^2}{\partial z^2}+\frac{1}{r^2}\right]\times A(\mathbf{r},t) \tag{16}$$

for the axial ones. A more comprehensive theory [37] gives the same result.

The relaxation law [Eq. (12)] is essentially a diffusion equation. Its eigenfunctions are overdamped: $P(\mathbf{r},t)=P(\mathbf{r},0)\exp(-t/\tau_P)$, $A(\mathbf{r},t)=A(\mathbf{r},0)\exp(-t/\tau_A)$ [38]. As usual, the spatial parts of the eigenmodes are factorized in $R(r)\Phi(\varphi)Z(z)$. Separation of variables shows that $\Phi(\varphi)$ is an arbitrary linear combination of $\sin m\varphi$ and $\cos m\varphi$ (m is an integer); similarly, any linear combination of $\sin k_3 z$ and $\cos k_3 z$ serves well for $Z(z)$. If both Ansätze are inserted in Eqs. (15) and (16) and if

$$\tau_P=\frac{\eta}{K(k_m^2+k_3^2)} \quad \text{and} \quad \tau_A=\frac{\eta}{K(k_{\sqrt{m^2-1}}^2+k_3^2)} , \tag{17}$$

where k_m and $k_{\sqrt{m^2-1}}$ are the radial components of the planar and axial fluctuation wave vectors, while k_3 is their axial component, the final amplitude equations for the radial parts of the planar and axial eigenmodes are obtained:

$$\left[\frac{\partial^2}{\partial r^2}+\frac{1}{r}\frac{\partial}{\partial r}+k_m^2-\frac{m^2}{r^2}\right]R_m(r)=0 \tag{18}$$

and

$$\left[\frac{\partial^2}{\partial r^2}+\frac{1}{r}\frac{\partial}{\partial r}+k_{\sqrt{m^2-1}}^2-\frac{m^2-1}{r^2}\right]R_{\sqrt{m^2-1}}(r)=0 . \tag{19}$$

These are Bessel equations, so the radial parts of both planar and axial eigenmodes are linear combinations of Bessel and Neumann functions of the order m and $\sqrt{m^2-1}$, respectively. The ratio of Bessel and Neumann functions in either the planar or axial eigenmode and its wave vector k_m (or $k_{\sqrt{m^2-1}}$) are determined by the boundary conditions. In the strong anchoring approach, the orientation of molecules is fixed by the solid surface, so the fluctuations should vanish there. Therefore,

$$R_m(r=R)=R_{\sqrt{m^2-1}}(r=R)=0 , \tag{20}$$

where R is the radius of the capillary. On the other hand, at the center of the capillary there is a line defect of strength $s=1$ where the nematic phase melts. Although the nematic order decreases gradually [39], not abruptly, one could describe the influence of the defect by a nematic-isotropic interface with an appropriate anchoring energy. However, the stability of the planar radial structure strongly depends on the type of anchoring at the defect as well [26]. In order to assure the existence of the structure at radii that correspond to capillaries of Anopore membranes, strong homeotropic anchoring at this interface—a rather artificial model—is assumed:

$$R_m(r=r_0)=R_{\sqrt{m^2-1}}(r=r_0)=0 , \tag{21}$$

where r_0 is the radius of the defect.

In a more complete treatment of anchoring, of the fluctuations the saddle-splay and splay-bend terms of the elastic free energy density ($-K_{24}\nabla\cdot[\mathbf{n}(\nabla\cdot\mathbf{n})+\mathbf{n}\times(\nabla\times\mathbf{n})]$ and $K_{13}\nabla\cdot[\mathbf{n}(\nabla\cdot\mathbf{n})]$, respectively) and the surface free energy—probably of the Rapini-Papoular form [40]—should be included. The defect's influence would be most properly taken into account by introducing a spatially modulated elastic constant, based on the order parameter profile [39], or even by a tensorial description. Still, we believe that our simple model already includes the basic physics of the fluctuations' dynamics, reducing the mathematical complexity.

Due to the boundary conditions, the spectrum of the radial components of the fluctuations' wave vectors k_m and $k_{\sqrt{m^2-1}}$ is discrete. An additional index l must be introduced to tag the wave vectors of the same order that give different number of zeros in the interval $[r_0,R]$. However, if the capillary is long enough, there is no selection rule for the axial wave vectors k_3.

The amplitude equation of the radial parts of the fluctuations' eigenmodes must be solved numerically. Some of them, corresponding to $r_0/R=0.05$, are shown in Fig. 4.

It turns out that for $r_0/R<0.0424$ there exist axial modes, solutions of Eq. (16), that do not have fluctuating character. The differential operator $-\nabla^2-1/r^2$ [the right-hand side of Eq. (16) divided by $-K$] is not positive definite. Its eigenvalues $\eta/K\tau_A=k_{\sqrt{m^2-1}}^2+k_3^2$ need not be positive. If $r_0/R<0.0424$, there is actually one negative $k_{\sqrt{m^2-1},l}^2$ (more precisely, $k_{i,0}^2$), giving rise to a range of negative values of $\eta/K\tau_A$. The eigenfunctions that correspond to the negative eigenvalues of the operator are exponentially *increasing* with time, not decaying as the fluctuations' eigenmodes. The critical value of the ratio r_0/R is in good agreement with the analytical result $e^{-\pi}\approx 0.0432\ldots$ [26]. The above indicates that in the one-constant approximation, the planar radial structure is stable only in rather small cylinders; if $r_0=5$ nm, the critical radius R_c of the capillary is approximately 116

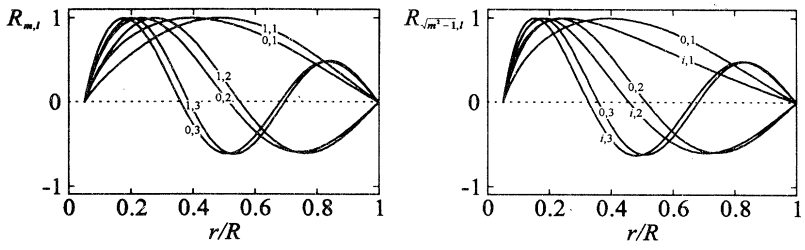

FIG. 4. Some of the radial parts of planar (a) and axial (b) modes, labeled by the indices k_m, l and $k_{\sqrt{m^2-1}}, l$ for a capillary with planar radial structure and $r_0=0.05R$. In both cases the y axis units are arbitrary.

nm. If the anchoring at the defect were not strong, the critical radius would be even smaller.

Once R_m and $R_{\sqrt{m^2-1}}$ are found, the fluctuating director field can be expanded in terms of its eigenmodes. The planar fluctuations

$$\mathcal{P}(\mathbf{r},t)=\sum_{Q}\sum_{i} p_i(Q)P_i(Q;\mathbf{r},t) , \tag{22}$$

where Q is used as a shorthand for (m,l,k_3). Functions $p_i(Q)$ are the amplitudes of the four planar eigenmodes $P_i(Q;\mathbf{r},t)$ with the same radial part but with different dependence on φ and z:

$$\begin{aligned}
P_1(Q;\mathbf{r},t)&=R_m(k_{m,l}r)\cos m\varphi\cos(k_3z)e^{-t/\tau_{P_1}(Q)} ,\\
P_2(Q,\mathbf{r},t)&=R_m(k_{m,l}r)\sin m\varphi\cos(k_3z)e^{-t/\tau_{P_2}(Q)} ,\\
P_3(Q;\mathbf{r},t)&=R_m(k_{m,l}r)\cos m\varphi\sin(k_3z)e^{-t/\tau_{P_3}(Q)} ,\\
P_4(Q;\mathbf{r},t)&=R_m(k_{m,l}r)\sin m\varphi\sin(k_3z)e^{-t/\tau_{P_4}(Q)} .
\end{aligned} \tag{23}$$

If $m=0$, $P_2(Q;\mathbf{r},t)=P_4(Q;\mathbf{r},t)\equiv 0$.

Similar series corresponds to the axial fluctuations:

$$\mathcal{A}(\mathbf{r},t)=\sum_{Q}\sum_{i} a_i(Q)A_i(Q;\mathbf{r},t) , \tag{24}$$

where $a_i(Q)$ and $A_i(Q;\mathbf{r},t)$ are just the axial counterparts of $p_i(Q)$ and $P_i(Q;\mathbf{r},t)$.

2. Rectangular model cavities

The mathematical description of order director fluctuations' eigenmodes [say, $X(\mathbf{r},t)$ and $Y(\mathbf{r},t)$] in uniform liquid crystal is much less complicated. In this case, $\lambda(\mathbf{r},t)=0$ and, as noted by de Gennes [29,36], they turn out to be

$$\begin{aligned}
\left.\begin{matrix}X(\mathbf{r},t)\\ Y(r,t)\end{matrix}\right\} \sim &\begin{Bmatrix}\cos k_x x\\ \sin k_x x\end{Bmatrix}\times\begin{Bmatrix}\cos k_y y\\ \sin k_y y\end{Bmatrix}\\
&\times\begin{Bmatrix}\cos k_z z\\ \sin k_z z\end{Bmatrix}\times\exp(-t/\tau) ,
\end{aligned} \tag{25}$$

where $\tau=\eta/K(k_x^2+k_y^2+k_z^2)$. The allowed wave vectors are determined by strong anchoring at the boundaries of the three rectangular model cavities, whereas in bulk nematic none of the three mutually perpendicular wave vectors k_x, k_y, and k_z is subjected to selection rules.

B. Frequency dependence of $\overline{J_h}(\omega)$

In order to calculate the spectral density $\overline{J_h}(\omega)$, the average square amplitude of the fluctuations' eigenmodes must be determined. In the one elastic constant approximation, the elastic energy is given by

$$\delta F=\frac{K}{2}\int[(\nabla\cdot\mathbf{n})^2+(\nabla\times\mathbf{n})^2]dV . \tag{26}$$

Now δF can be expanded in terms of $\delta\mathbf{n}$: zeroth order terms correspond to the equilibrium free energy, first order terms vanish upon integration because the equilibrium structure is an extreme of the free energy, and second order terms represent the order director fluctuations' elastic free energy.

1. Cylindrical capillary

For the cylindrical capillary with planar radial structure,

$$\begin{aligned}
\delta F=\frac{K}{2}\int\Bigg\{&\left[\frac{\partial\mathcal{P}}{\partial r}\right]^2+\frac{1}{r^2}\left[\frac{\partial\mathcal{P}}{\partial\varphi}\right]^2+\left[\frac{\partial\mathcal{P}}{\partial z}\right]^2\\
&+\frac{2}{r}\left[\frac{\partial\mathcal{P}}{\partial\varphi}\frac{\partial\mathcal{A}}{\partial z}-\frac{\partial\mathcal{P}}{\partial z}\frac{\partial\mathcal{A}}{\partial\varphi}\right]+\left[\frac{\partial\mathcal{A}}{\partial r}\right]^2\\
&-\frac{2\mathcal{A}}{r}\frac{\partial\mathcal{A}}{\partial r}-\frac{\mathcal{A}^2}{r^2}+\frac{1}{r^2}\left[\frac{\partial\mathcal{A}}{\partial\varphi}\right]^2\\
&+\left[\frac{\partial\mathcal{A}}{\partial z}\right]^2\Bigg\}dV ,
\end{aligned} \tag{27}$$

where $\mathcal{P}=\mathcal{P}(\mathbf{r},t)$ and $\mathcal{A}=\mathcal{A}(\mathbf{r},t)$. Note that if all second order terms of δF are to be collected, the fluctuation director must also be expanded up to second order $\delta\mathbf{n}=(-\frac{1}{2}\mathcal{P}^2-\frac{1}{2}\mathcal{A}^2,\mathcal{P},\mathcal{A})$.

Next, the planar and axial fluctuations' expansions, Eqs. (22) and (24), are introduced into Eq. (27) and the integration over the volume of the nematic phase is performed. Evaluation of integrals over $\varphi\in[0,2\pi]$ and $z\in[-L/2,L/2]$ is straightforward; it is assumed that terms of the form in Eq. (27)

$$\cdots[p_1^2(Q)+p_2^2(Q)-p_3^2(Q)-p_4^2(Q),]\sin k_3L , \tag{28}$$

corresponding to the two mixed terms, cancel upon summation over Q. The amplitudes $p_i(Q)$ vary only smoothly with Q, while the phase $\sin k_3L$ oscillates. Besides, the thermal averages of $p_i^2(Q)$ turn out to be equal, so that the thermal average of the sum in the brackets—which actually has to be calculated—vanishes anyway.

Equation (27) is thus expressed as

$$\delta F=\frac{\pi KL}{4}\sum_{\mathcal{Q}}\{[p_1^2+p_2^2+p_3^2+p_4^2][\alpha_{m,l}+(k_3R)^2\beta_{m,l}] +[a_1^2+a_2^2+a_3^2+a_4^2] \times[\gamma_{m,l}+(k_3R)^2\delta_{m,l}]\}\ , \tag{29}$$

where $p_i=p_i(\mathcal{Q})$ and $a_i=a_i(\mathcal{Q})$ and

$$\begin{aligned}
\alpha_{m,l}&=\int_{r_0}^{R}\left[(R_m')^2r+\frac{m^2}{r}R_m^2\right]dr\ ,\\
\beta_{m,l}&=\frac{1}{R^2}\int_{r_0}^{R}rR_m^2dr\ ,\\
\gamma_{m,l}&=\int_{r_0}^{R}\left[(R'_{\sqrt{m^2-1}})^2r-2R'_{\sqrt{m^2-1}}R_{\sqrt{m^2-1}}+\frac{m^2-1}{r}R^2_{\sqrt{m^2-1}}\right]dr\ ,\\
\delta_{m,l}&=\frac{1}{R^2}\int_{r_0}^{R}rR^2_{\sqrt{m^2-1}}dr
\end{aligned} \tag{30}$$

with $R_m=R_m(k_{m,l}r)$ and $R_{\sqrt{m^2-1}}=R_{\sqrt{m^2-1}}(k_{\sqrt{m^2-1},l}r)$; primes denote $\partial/\partial r$.

According to the equipartition theorem, the average square amplitude of a planar fluctuation mode is

$$\langle p_i^2(\mathcal{Q})\rangle=\frac{2kT}{\pi KL[\alpha_{m,l}+(k_3R)^2\beta_{m,l}]}\ . \tag{31}$$

where $i=1,2,3,4$ and $m>0$. For $m=0$, $\langle p_1^2(\mathcal{Q})\rangle=\langle p_3^2(\mathcal{Q})\rangle$ is just twice as large, while $\langle p_2^2(\mathcal{Q})\rangle=\langle p_4^2(\mathcal{Q})\rangle=0$. But since the spectral density only depends on the *sum* of the contributions of the four P_i's—which equals $8kT/\pi KL[\alpha_{m,l}+(k_3R)^2\beta_{m,l}]$ for all m—no distinction between the cases $m=0$ and $m>0$ will be made.

Now the spectral density of the autocorrelation functions Eq. (7) can be evaluated. Introducing Eq. (22) in Eq. (7) gives terms of the form

$$\overline{J_h^P}(\omega)=g_h(\alpha)S^2\sum_{\mathcal{Q}}\sum_i\int_{-\infty}^{\infty}\overline{\langle p_i^2(\mathcal{Q})\rangle P_i^2(\mathcal{Q};\mathbf{r})}e^{-t/\tau_{P_i}(\mathcal{Q})}e^{-i\omega t}dt\ , \tag{32}$$

where $\overline{J_h^P}(\omega)$ is the contribution of the planar fluctuations to the total spectral density. Integrating over time and averaging over the capillary yields

$$\overline{J_h^P}(\omega)=g_h(\alpha)S^2\sum_{\mathcal{Q}}\sum_i\frac{\beta_{m,l}}{[1-(r_0/R)^2]}\langle p_i^2(\mathcal{Q})\rangle\frac{\tau_{P_i}(\mathcal{Q})}{1+\omega^2\tau^2_{P_i}(\mathcal{Q})}\ . \tag{33}$$

The four terms corresponding to $P_1(\mathcal{Q};\mathbf{r})$, $P_2(\mathcal{Q};\mathbf{r})$, $P_3(\mathcal{Q};\mathbf{r})$, and $P_4(\mathcal{Q};\mathbf{r})$ turn out to be equal. Using Eq. (31), the planar fluctuations' spectral density becomes

$$\overline{J_h^P}(\omega)=\frac{4kTS^2\eta R^2}{\pi(1-\rho^2)K^2L}g_h(\alpha)\sum_{\mathcal{Q}}\frac{\beta_{m,l}}{\alpha_{m,l}+(k_3R)^2\beta_{m,l}}\frac{(k_{m,l}R)^2+(k_3R)^2}{[(k_{m,l}R)^2+(k_3R)^2]^2+\Omega^2}\ , \tag{34}$$

Since there is no selection rule for axial components of the fluctuations' wave vectors, the triple sum (over m,l and k_3) can be integrated over k_3. The capillary is assumed to be very long, so the lower limit of the integral is set to 0. The upper limit is determined by the size of the molecule: the wavelength of the axial modulation of an eigenmode must be larger than, say, $4d$ (where d is the thickness of the molecule). Therefore, $k_3<\pi/2d=\lambda/R$. Finally,

$$\begin{aligned}
\overline{J_h^P}(\omega)=&\frac{2kTS^2\eta R}{\pi^2(1-\rho^2)K^2}g_h(\alpha)\\
&\times\sum_{m,l}\frac{\beta}{\alpha^2-2\alpha\beta\kappa^2+\beta^2\kappa^4+\beta^2\Omega^2}\\
&\times\left\{\left[\frac{\beta}{\alpha}\right]^{1/2}(\beta\kappa^2-\alpha)\arctan\left[\left[\frac{\beta}{\alpha}\right]^{1/2}\lambda\right]\right.\\
&+\frac{1}{2\sqrt{2}C}\left\{\frac{\alpha\kappa^2-\beta\kappa^4+\beta\Omega^2+(\alpha-\beta\kappa^2)C}{\sqrt{C+\kappa^2}}\left[\arctan\left[\frac{\sqrt{2}\lambda-\sqrt{C-\kappa^2}}{\sqrt{C+\kappa^2}}\right]+\arctan\left[\frac{\sqrt{2}\lambda+\sqrt{C-\kappa^2}}{\sqrt{C+\kappa^2}}\right]\right]\right.\\
&\left.\left.+\frac{\sqrt{C-\kappa^2}(\alpha-2\beta\kappa^2-\beta C)}{2}\ln\left|\frac{-\lambda^2+\lambda\sqrt{2}\sqrt{C-\kappa^2}-C}{\lambda^2+\lambda\sqrt{2}\sqrt{C-\kappa^2}+C}\right|\right\}\right\}\ ,
\end{aligned} \tag{35}$$

with $\kappa=k_{m,l}R$ and $C=\sqrt{\kappa^4+\Omega^2}$. Indices m and l in $\alpha_{m,l}$ and $\beta_{m,l}$ were omitted for clarity. The density of states in the reciprocal space of wave vector k_3, $L/2\pi$ is taken into account. The sum should include all the fluctuations' modes for which the smallest distance between the adjacent zeros of the radial parts of the eigenfunctions is larger than two molecular lengths. As expected, the spectral density does not depend on the length of the capillary. A similar expression is found for the axial fluctuations' contributions to the spectral density.

2. *Rectangular model cavities*

In the case of uniform nematic liquid crystals in rectangular model cavities, the analysis is analogous. The spectral density $J_h(\omega)$ for the uniform nematic liquid crystal is [7]

$$J_h(\omega)=\frac{8kTS^2\eta}{VK^2}g_h(\Delta)\sum_q\frac{1}{q^4+\omega^2\eta^2/K^2}\ , \tag{36}$$

which, if the denominator and the numerator are multiplied by R^4, becomes

$$J_h(\omega)=\frac{8kTS^2\eta R^4}{VK^2}g_h(\Delta)\sum_q\frac{1}{(qR)^4+\Omega^2}\ , \tag{37}$$

where V is the volume of the sample, Δ is the angle between the director and the magnetic field, and q is the length of the wave vector of the bulk fluctuations' eigenmodes, corresponding to $\sqrt{k_{m,l}^2+k_3^2}$ and $\sqrt{k^2_{\sqrt{m^2-1},l}+k_3^2}$. The difference between the above expression and Eq. (34) is due to different average square amplitudes of an eigenmode in the uniform and planar radial configurations. The former is just kT/Kq^2V [7] (which is proportional to the decay time of an eigenmode $\tau=\eta/Kq^2$) and the latter is given by Eq. (31). The characteristic factor $1/[(qR)^4+\Omega^2]$ appears in both spectral densities. Again, the summation over wave vectors that are not subjected to selection rules can be replaced by an integral.

C. Angular dependence of $\overline{J_h}(\omega)$

In the next step, the orientation-dependent parts of the correlation functions $\langle\mathcal{F}_h(0)\mathcal{F}_h^*(t)\rangle$ are calculated. If the axis of the capillary is put in plane yz of the laboratory reference frame Σ, the director field is described by

$$\mathbf{n}=(\cos\phi,\cos\alpha\sin\phi,-\sin\alpha\sin\phi)\ , \tag{38}$$

where α is the angle between the capillary's axis and the magnetic field, which coincides with the z axis (Fig. 3). The angular dependences of the correlation functions are given by Eqs. (8). Angle θ—one of the parameters of the Euler rotation from Σ to Σ'—depends on azimuthal angle ϕ, which parametrizes the rotation as well. Angular averaging in Eqs. (8) is therefore reduced to ϕ [although it enters Eqs. (8) only indirectly, through θ] and ψ. In the latter case, uniaxial symmetry of the nematic phase is reflected through invariance of the orientation of axes x' and y' in the laboratory coordinate system.

To evaluate Eqs. (8) in terms of α, it is sufficient to compute $\cos\theta$ as a function of ϕ. Taking the dot product of $\mathbf{n}$ [Eq. (38)] and the unit vector parallel to the z axis yields $\cos\theta=-\sin\alpha\sin\phi$. Assuming the molecular diffusion in the capillary is fast enough, the averaging over $\psi\in[0,2\pi]$ and $\phi\in[0,2\pi]$ in Eqs. (8) can be performed, giving

$$\begin{aligned}g_0(\alpha)&=\tfrac{9}{4}(1+2\cos^2\alpha-3\cos^4\alpha)\ ,\\ g_1(\alpha)&=\tfrac{1}{4}(2-3\cos^2\alpha+3\cos^4\alpha)\ ,\\ g_2(\alpha)&=\tfrac{1}{4}(5+6\cos^2\alpha-3\cos^4\alpha)\ .\end{aligned} \tag{39}$$

The resultant angular dependences of the spectral densities are presented in Fig. 5. [The function $g_0(\alpha)$ is not important in the order director fluctuations' T_1^{-1}, but we cite it because it enters the spin-lattice relaxation rate in the rotating frame and the spin-spin relaxation rate T_2^{-1}.] It is instructive to compare the capillary's g_hs with their uniform counterparts [7] [Fig. 5(b)]:

$$\begin{aligned}g_0(\Delta)&=18(\cos^2\Delta-\cos^4\Delta)\ ,\\ g_1(\Delta)&=\tfrac{1}{2}(1-3\cos^2\Delta+4\cos^4\Delta)\ ,\\ g_2(\Delta)&=2(1-\cos^4\Delta)\ ,\end{aligned} \tag{40}$$

where Δ denotes the angle between the nematic director and the magnetic field. Note that $g_h(\alpha=0)=g_h(\Delta=\pi/2)$ as it should be, because in these cases both director fields are perpendicular to the magnetic field.

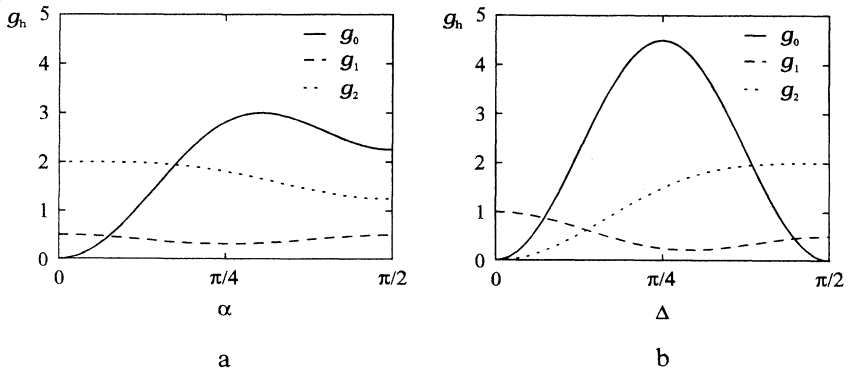

FIG. 5. Angular dependence of the spectral densities in planar radial structure (a) and uniform nematic structure (b). The functions g_h depend on the angle between the axis of the capillary and the magnetic field and the angle between the uniform director and the magnetic field, respectively. Note that $g_1(\alpha)$ and $g_2(\alpha)$ are more moderate than their uniform counterparts $g_1(\Delta)$ and $g_2(\Delta)$.

III. RESULTS

A. Cylindrical capillaries

The frequency dependence of the planar fluctuation spectral density in the capillary with planar radial structure is given by Eq. (35). Let us first examine its asymptotic behavior. In the limit of low frequencies ($\omega \ll \eta R^2/K$) the spectral density (and, therefore, the relaxation rate) is finite and frequency independent, while at high frequencies ($\omega \gg \eta x^2/K$, where x is the length of the nematic molecule)

$$\overline{J_h^P}(\omega \to \infty) \propto \frac{1}{\omega^2} . \tag{41}$$

Both limits coincide with earlier models [7–12] and experimental data [7,14,41] as well.

In Fig. 6, the spin-lattice relaxation rate of the nematic in capillaries with $R=20$, 60, 100, 110, and 115 nm is shown. The capillary with $R=100$ nm corresponds to cylindrical cavities in Anopore membranes which, filled with nematic liquid crystals, were extensively studied using various experimental techniques [22,23,42,43], and the radius of the largest capillary is just below the critical radius where the structural transition should occur. The radius of the defect is taken equal to 5 nm and the minimal allowed wavelength of R_m and $R_{\sqrt{m^2-1}}$ is set to 4 molecular lengths (~ 8 nm), while for the axial modulation it is five times smaller—if it is assumed that the thickness of the molecule equals one fifth of its length. The values of other parameters are $T=293$ K, $S=0.4$, $b=0.2$ nm, $K=10^{-11}$ N, and $\eta=0.01$ N s m^{-2}. The capillaries are parallel to the magnetic field.

In capillaries with $R \leq 100$ nm the dispersion of the relaxation rate can be divided into three regimes. At low frequencies, T_1^{-1} is constant, as was already inferred directly from Eq. (35). The lower critical frequency, which separates the low-frequency regime and the bulk $\nu^{-1/2}$ dependence, is determined by the size of the capillary; it decreases with increasing capillary diameter. In the MHz range, the relaxation rate in the larger capillaries ($R=60,100,110,115$ nm) obeys the bulk law. At high frequencies all curves match.

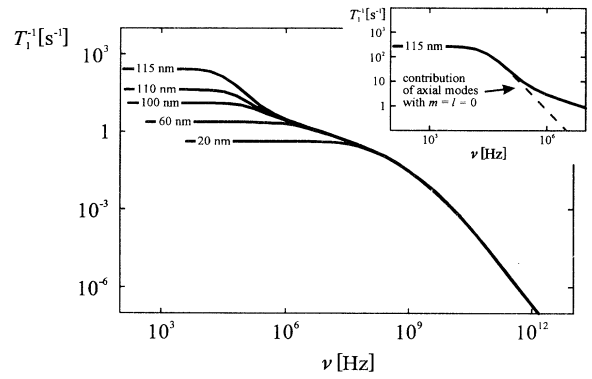

FIG. 6. Frequency dependence of the relaxation rate T_1^{-1} in capillaries with $R=20$, 60, 100, 110, and 115 nm, parallel to the magnetic field. The parameters used in the calculation are $T=293$ K, $S=0.4$, $K=10^{-11}$ N, $\eta=0.01$ N s m^{-2}, $b=0.2$ nm, $r_0=5$ nm; the length of the molecules is taken to be 2 nm. At larger radii, the low-frequency behavior is almost entirely due to the slowest axial modes, corresponding to $m=l=0$ (inset).

In the vicinity of the structural transition ($R=110$ and 115 nm), the low-frequency behavior is modified. Again, $T_1^{-1}(\nu \to 0)$ does not depend on frequency, but it is considerably increased with respect to the 100 nm capillary. In addition, the low-frequency plateau and the bulk $\nu^{-1/2}$ law are separated by a transient regime. Just below the structural transition ($R=115$ nm) the transient regime is characterized by a ν^{-2} dependence. This indicates that the relaxation rate is dominated by a single mode: frequency dependence of a single mode's contribution to the spectral density [Eq. (33)] is given by

$$\frac{\tau}{1+\omega^2\tau^2} \tag{42}$$

where $\tau=\tau_{P_i}(Q)$ or $\tau_{A_i}(Q)$. The dominating mode is obviously the one with the largest average square amplitude. There are two such modes: $A_1((m=0,l=0,k_3=0);\mathbf{r},t)$ and $A_3((m=0,l=0,k_3=0);\mathbf{r},t)$. (For $R>116$ nm, these two are responsible for the transition to the escaped structure.) Their average square amplitude is (for $r_0/R=5$ nm/115 nm$=0.0435$, $\gamma_{0,0}=7.509\times10^{-3}$; $L=60$ μm as in Anopore membranes)

$$\langle a_1^2(0,0,0)\rangle = \langle a_3^2(0,0,0)\rangle = \frac{4kT}{\pi K L \gamma_{0,0}} = 1.14\times10^{-3} , \tag{43}$$

which indicates that the deflections from the equilibrium director are still rather small. However, the average square amplitude [Eq. (31)] and the relaxation time [Eq. (17)] of a mode do not change much if k_3 is finite but small. Therefore, the low-frequency behavior in the vicinity of the structural transition, should be attributed to all axial modes with $m=l=0$. Indeed, as shown in the inset of Fig. 6, these account for the greater part of the low-frequency relaxation rate (more precisely, 98.8%). For the above set of material and geometrical parameters, above ~ 1 MHz the relaxation rate obeys the Pincus dispersion and for $\nu > 10$ GHz, $T_1^{-1} \propto \nu^{-2}$.

Apparently, the three regimes exhibited by the nematic order director fluctuations in a capillary with $R \leq 100$ nm are generally the same as in bulk nematic. The high-frequency ν^{-2} dependence corresponds to the absence of fluctuation modes with very short wavelengths that is due to the finite size of the nematic molecule and, therefore, is geometry independent. The low-frequency plateau is caused by the lack of the ultralong wavelength fluctuations. In case of microconfined systems, their wavelength must be smaller than the size of the cavity, while in bulk nematic liquid crystal they are determined by the dimension of a uniformly oriented domain. In what way do the shape of the confining cavity and the nematic structure affect the order director fluctuations' nuclear spin relaxation if the size of the cavity is far from the critical? In order to answer this intriguing question, the results are compared to the relaxation rate of uniformly oriented nematic liquid crystals in the three model cavities.

B. Rectangular model cavities

The rectangular model cavity relaxation rates are presented in Fig. 7. The characteristic size X of the rectangular cavities (i.e., the side of the cube, the side of the waveguide's cross section, and the thickness of the sandwich) matches the radius of the capillary. The model cavities are oriented so that the director fields are perpendicular to the magnetic field. Again, two sets of dispersion relations are shown, one for $X=20$ nm and one for $X=100$ nm. The material constants and the temperature are the same as in Fig. 6. The relaxation rates of 20 and 100 nm capillaries are replotted to facilitate the comparison.

In all three cases, not depending on the dimensionality of the confinement, the relaxation rate exhibits basically the same behavior: plateau at low frequencies, classical bulk $\nu^{-1/2}$ dependence in the MHz range, and the ν^{-2} regime at high frequencies. The dispersion relations of the whole set differ at low frequencies only, where T_1^{-1} is largest in the layer and smallest in the cube. The relaxation rate of the larger capillary is somewhat larger than that of the thicker layer, while T_1^{-1} of capillary with $R=20$ nm is smaller than the relaxation rate of cube with $X=20$ nm. The curves eventually merge in the MHz range.

Comparison of the two sets shows that the onset of the low-frequency plateau depends on the characteristic size of the cavity. The larger than size, the lower the onset of the plateau.

C. Confinement and orientational dependence of T_1^{-1}

So far, we have studied only the effect of confinement on the frequency dependence of the relaxation rate. For the particular orientation of the capillary (parallel to the magnetic field) it is possible to compare the capillary's relaxation rate to the T_1^{-1}, corresponding to uniformly aligned nematic liquid crystal in rectangular model cavities, perpendicular to **B**. It is, however, interesting to examine the orientational dependence of the relaxation rate in a confined sample as well.

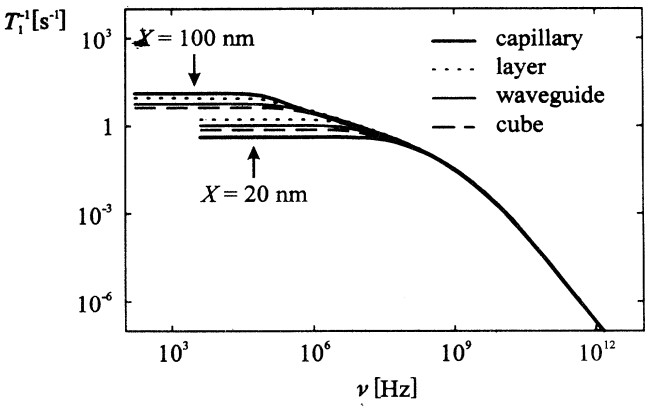

FIG. 7. Frequency dependence of T_1^{-1} in the rectangular model systems with characteristic size 20 and 100 nm. Other parameters are the same as in Fig. 6. Uniform nematic structures in the three model cavities are perpendicular to the magnetic field. The relaxation rates in the capillaries with $R=20$ and 100 nm are replotted to facilitate the comparison.

In Fig. 8 the ratio of $T_1^{-1}(\Delta)/T_1^{-1}(0)$ for a layer with a thickness of 2 μm is shown as a function of frequency and the angle between the normal of the layer and the magnetic field. (The material constants and the temperature are the same as before.) The ratio clearly exhibits steplike behavior, corresponding to the three regimes. At low frequencies the relaxation rate increases by a factor of 2.5 as Δ goes from 0 to $\pi/2$. When the same rotation is performed at intermediate frequencies (in the range of the classical $\nu^{-1/2}$ law), T_1^{-1} is approximately doubled. Finally, at high frequencies the relaxation rate shows nonmonotonous dependence on Δ. The high-frequency behavior is related to the finite size of the nematic molecules, but the low-frequency behavior is entirely due to the confinement. If the thickness of the layer is increased, the lower critical frequency decreases; in a monodomain uniform bulk sample it should approach 0.

In case of a cylindrical cavity with planar radial nematic structure, the relaxation rate's dependence on the angle between the axis of the capillary and the magnetic field turns out to be qualitatively similar (i.e., steplike) but, unless $R \sim R_c$, less pronounced. This is not surprising, since functions $g_1(\alpha)$ and $g_2(\alpha)$ [Eqs. (39)] are more moderate than their counterparts corresponding to uniform structure.

Thus, the typical sizes of the confining cavity and the nematic molecule can be estimated using the dispersion relation $T_1^{-1}(\nu)$ at fixed orientation of the sample with respect to the magnetic field. On the other hand, measurements of the orientational dependence of T_1^{-1} at fixed frequency could serve as a method of identification of the liquid crystalline structures—an alternative and a complement to the widely used NMR, where the absorption spectrum is closely related to the nematic configuration.

IV. DISCUSSION

The calculated dispersion curves for the relaxation rates T_1^{-1} of a nematic in the cylindrical cavity, cube, waveguide, and sandwich are similar, in particular the three that belong to the rectangular geometries. The

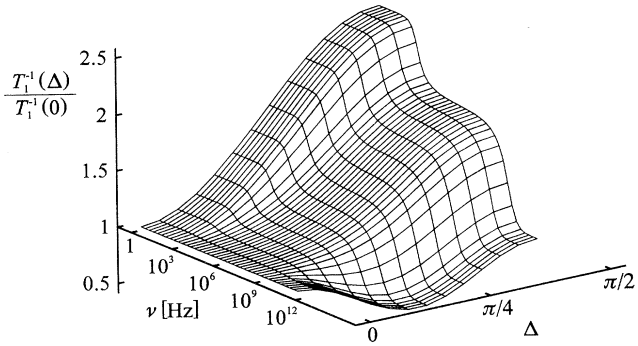

FIG. 8. $T_1^{-1}(\Delta)/T_1^{-1}(0)$ for the layer with thickness 2 μm as a function of frequency and angle between the normal of the layer and the magnetic field. The low-frequency behavior is characteristic of the confined samples.

effect of the confinement is rather small. A nematic restricted to a cube is, no doubt, a physical system substantially different from those in an infinite waveguide and an infinite sandwich. But when the order director fluctuations are considered, they share a fundamental feature as shown below.

Knowing that the low-frequency plateau is caused by the lack of long wavelength fluctuations, it is reasonable to examine the fluctuations' spectra in the three geometries. Each eigenmode's wave vector is decomposed into three orthogonal components, one longitudinal and two transverse with respect to the director. According to the boundary conditions, in the sandwich there exists a selection rule for the perpendicular component k_z of the eigenmode's wave vector; the two in-plane components k_x and k_y are free from boundary conditions. Therefore, the spectrum of the bound component of the fluctuation mode is discrete $k_z = n\pi/2X$ (where n is an integer and X the thickness of the layer), while the other two components can be varied continuously. Now, k_z cannot be 0, since the eigenmode in this case vanishes. So there is a lower limit of the perpendicular component of the fluctuation's mode wave vector. Since $q^2 = k_x^2 + k_y^2 + k_z^2$, the smallest q corresponds to the smallest k_z and $k_x = k_y = 0$. Therefore, the overall spectrum is limited both downward and upward (the upper limit is defined by the size of the molecule, which determines the minimum scale of validity of the continuum model).

A similar argument applies in the case of a waveguide-like cavity with two discrete and one continuous component of the eigenmodes' wave vectors. The lower limit of the spectrum is $q_{\min} = \sqrt{k_{x,\min}^2 + k_{y,\min}^2}$, where k_x and k_y are the bound components of the wave vectors. When the nematic cube is considered, $q_{\min}$ equals $\sqrt{k_{x,\min}^2 + k_{y,\min}^2 + k_{z,\min}^2}$. Thus, if the nematic liquid crystal is confined to a cavity, there always exists a lower limit of the fluctuation spectrum, no matter how many spatial dimensions are restricted. Generally, the relaxation rate does not depend on whether or not the spectrum itself is continuous, which can also be inferred from Fig. 7. Its cutoff frequencies, which separate the three regimes, merely reflect the typical macroscopic and microscopic sizes of the sample.

The above discussion suggests that the ratio of lower limits of the fluctuation spectra in the cube, the waveguide, and the layer with the same characteristic size should equal $\sqrt{3}:\sqrt{2}:1$ if the thickness of the nematic molecule is taken to be equal to its length. On the other hand, if the ratio of the characteristic sizes of the three model systems is $\sqrt{3}:\sqrt{2}:1$, the lower limits of the spectra are equal. In this case, the dispersion relations are even closer (Fig. 9). At low frequencies, the relaxation rate in the waveguide is about 10% larger than in the cube and approximately 10% smaller than in the layer. Again, the curves merge in the MHz range.

Finally, a remark must be made on the integration volume belonging to the allowed fluctuation modes. As already mentioned, the eigenmode's wave vector is decomposed into three mutually perpendicular components—say, k_x, k_y, and k_z—that are subjected to

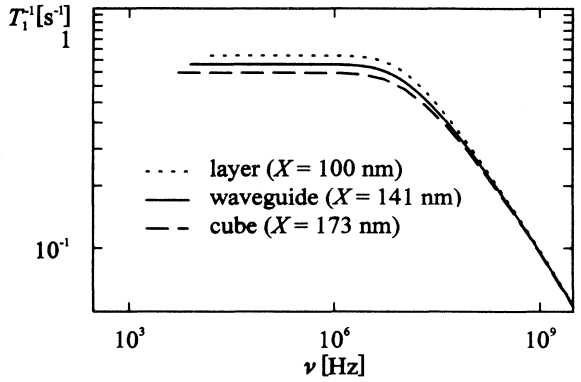

FIG. 9. Dispersion in rectangular model systems with equal lower limits of the fluctuation spectra. The side of the cube equals 173 nm, the side of the cross section of the waveguide 141 nm, and the thickness of the layer 100 nm.

selection rules, if the liquid crystal is restricted in the corresponding directions x, y, and z. In the case of the nematic cube, for instance, $k_x = n\pi/2d$, $n = 1, \ldots, n_{\max}$, where $n_{\max} \sim X/x$ (X is the side of the cube); similar relations determine the ranges of k_y and k_z. So, if the summation over discrete values of k_x, k_y, and k_z is to be replaced by an integral, the integration volume should be blocklike: $[k_{x,\min}, k_{x,\max}] \times [k_{y,\min}, k_{y,\max}] \times [k_{z,\min}, k_{z,\max}]$. More precisely, the integration volume is tetragonal because of uniaxial symmetry of the nematic phase. In the same manner, one finds that the integration volumes corresponding to the fluctuation modes in the waveguide and sandwich simply retain the shape of the confining cavity.

So far, the integration volume in the reciprocal space has usually been a sphere [6,7], a cylinder [9,10], or a rotational ellipsoid [11]. In these cases the spectral density can be expressed analytically. In Fig. 10 the relaxation rates calculated by spherical approximation with both short- and long-wavelength cutoffs (where the integration volume is essentially a coreless sphere) and by discrete summation over the eigenmodes of a cube are compared

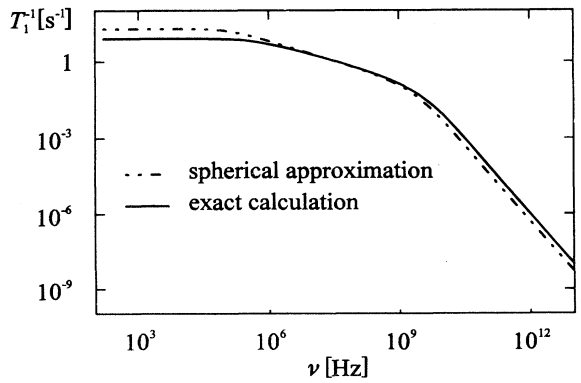

FIG. 10. Comparison of the relaxation rates, calculated by spherical approximation and by discrete summation over fluctuation eigenmodes in the cube. The spherical approximation gives somewhat larger relaxation rates at low frequencies and a bit smaller values at high frequencies.

for $X=200$ nm and *the same* minimal and maximal fluctuations' wavelengths. Generally, the two dispersion curves are similar, yet they differ slightly: at low frequencies, the spherical approximation gives a somewhat higher relaxation rate, while at high frequencies it predicts a bit smaller T_1^{-1}. In our opinion, by adjusting the short- and long-wavelength cutoffs of the spherical approximation, the relaxation rate computed in this simple way can be brought quite close to the exact calculation. It is, therefore, reasonable to replace the cubelike fluctuation spectrum with the coreless sphere (or, if the elongated shape of the nematic molecules is taken into account, the tetragonal one with the coreless rotational ellipsoid).

V. CONCLUSIONS

The order director fluctuations of a nematic liquid crystal confined to a cylindrical capillary with planar radial structure and rectangular model cavities, confined in three, two, and one spatial dimension, are studied within Frank elastic theory. The confining geometries, some rather unnatural, allow transparent analysis of the influence of confinement on the fluctuations' spin-lattice relaxation rates. The dispersion relation $T_1^{-1}=T_1^{-1}(\nu)$ is obtained numerically for each of the nematic systems.

The main result of the study is the proof that at low frequencies the order direction fluctuations' spin-lattice relaxation rates are frequency independent, no matter how many dimensions of a confined nematic liquid crystal are restricted. In the MHz range the relaxation rate obeys Pincus's $\nu^{-1/2}$ law and at high frequencies $T_1^{-1}\propto\nu^{-2}$.

The effects of the shape of the cavity and the imposed structure on the dispersion relation are rather limited. The onset of the low-frequency plateau is generally determined by the size of the confining cavity. However, in the vicinity of a structural transition, if it is allowed in the particular geometry, $T_1^{-1}(\nu<10^5$ Hz) is considerably increased and the low-frequency behavior is strongly dominated by the slowest modes. In real systems such a transition can be induced, for instance, by changing the temperature, since the elastic constants are temperature-dependent. The angular dependence of the relaxation rate is characteristic for the nematic configuration.

Recently [44], spin-lattice relaxation rate measurements were performed on 5CB in untreated anopore membrane, where the molecules were oriented along the symmetry axis of the capillaries. The experiment, carried out on a powerful field-cycling spectrometer with a broad frequency range [41], did not reveal any significant difference between bulk and confined samples, which is consistent with our conclusions. Further measurements with treated membranes, where the planar polar director configuration is expected [Fig. 1(b)], are planned [45]. However, preliminary calculations concerning the order director fluctuations in the planar polar configuration indicate substantial mathematical complexity of the problem.

ACKNOWLEDGMENTS

We thank Professor P. Palffy-Muhoray for helpful discussions and for sending us some of his recent results before publication. Support from the Ministry of Science and Technology of Slovenia (Grant No. P1-5034-0790-94) is acknowledged.

[1] P. Pincus, Solid State Commun. **7**, 415 (1969).
[2] R. Blinc, D. L. Hogenboom, D. E. O'Reilly, and E. M. Peterson, Phys. Rev. Lett. **23**, 969 (1969).
[3] W. Wölfel, F. Noack, and M. Stohrer, Z. Naturforsch. Teil A **30**, 437 (1975).
[4] W. Wölfel, *Kernrelaxationsuntersuchungen der Molekülbewegung im Flüssigkristal PAA* (Minerva Publikation, München, 1978).
[5] Th. Mugele, V. Graf, F. Noack, and M. Stohrer, Z. Naturforsch. Teil A **35**, 924 (1980).
[6] P. Ukleja, J. Pirš, and J. W. Doane, Phys. Rev. A **14**, 414 (1976).
[7] J. W. Doane, C. E. Tarr, and M. A. Nickerson, Phys. Rev. Lett. **33**, 620 (1974).
[8] R. Blinc, M. Vilfan, and V. Rutar, Solid State Commun. **17**, 171 (1975).
[9] R. Blinc, M. Luzar, M. Vilfan, and M. I. Burgar, J. Chem. Phys. **63**, 3445 (1975).
[10] R. Blinc, NMR: Basic Princ. Prog. **13**, 97 (1976).
[11] R. R. Vold and R. L. Vold, J. Chem. Phys. **88**, 4655 (1988).
[12] A. C. Ribeiro, P. S. Sebastiao, and M. Vilfan, Liq. Cryst. **3**, 937 (1988), and references therein.
[13] J. W. Doane, N. A. Vaz, B. G. Wu, and S. Žumer, Appl. Phys. Lett. **48**, 4 (1986).
[14] R. E. Dong, *Nuclear Magnetic Resonance of Liquid Crystals* (Springer-Verlag, Berlin, 1994).
[15] A. Golemme, S. Žumer, D. W. Allender, and J. W. Doane, Phys. Rev. Lett. **61**, 2937 (1988).
[16] M. Vilfan, V. Rutar, S. Žumer, G. Lahajnar, R. Blinc, J. W. Doane, and A. Golemme, J. Chem. Phys. **89**, 597 (1988).
[17] J. Dolinšek, O. Jarh, M. Vilfan, S. Žumer, R. Blinc, J. W. Doane, and G. P. Crawford, J. Chem. Phys. **95**, 2154 (1991).
[18] S. Žumer, M. Vilfan, and I. Vilfan, Liq. Cryst. **3**, 947 (1988).
[19] G. P. Crawford, M. Vilfan, J. W. Doane, and I. Vilfan, Phys. Rev. A **43**, 835 (1991).
[20] G. P. Crawford, D. W. Allender, J. W. Doane, M. Vilfan, and I. Vilfan, Phys. Rev. A **44**, 2570 (1991).
[21] R. J. Ondris-Crawford, G. P. Crawford, S. Žumer, and J. W. Doane, Phys. Rev. Lett. **70**, 194 (1993).
[22] G. P. Crawford, R. J. Ondris-Crawford, S. Žumer, and J. W. Doane, Phys. Rev. Lett. **70**, 1838 (1993).
[23] N. Vrbančič, M. Vilfan, R. Blinc, J. Dolinšek, G. P. Crawford, and J. W. Doane, J. Chem. Phys. **98**, 3540 (1993).
[24] See, for instance, M. Vilfan and S. Žumer, Croatica Chem. Acta **65**, 327 (1992).
[25] P. E. Cladis, M. Kléman, J. Phys. (France) **33**, 591 (1972).
[26] P. Palffy-Muhoray, A. Sparavigna, and A. Strigazzi, Liq. Cryst. **14**, 1143 (1993).

[27] R. J. Ondris-Crawford, G. P. Crawford, J. W. Doane, S. Žumer, M. Vilfan, and I. Vilfan, Phys. Rev. E **48**, 1998 (1993).
[28] P. G. de Gennes, Mol. Cryst. 7, 325 (1969).
[29] Groupe d'Etude des Cristaux Liquides (Orsay), J. Chem. Phys. **51**, 816 (1969).
[30] A. Abragam, *Principles of Nuclear Magnetism* (Oxford University Press, Oxford, 1967).
[31] K. Kohlhammer, K. Müller, and G. Kothe, Liq. Cryst. **5**, 1525 (1989).
[32] J. W. Doane and D. L. Johnson, Chem. Phys. Lett. **6**, 291 (1970).
[33] S. Chandrasekhar, *Liquid Crystals* (Cambridge University Press, Cambridge, 1992).
[34] M. Čopič, and N. A. Clark, Liq. Cryst. **17**, 149 (1994).
[35] L. D. Landau and I. M. Halatnikov, Dokl. Akad. Nauk SSSR **96**, 469 (1954).
[36] P. G. de Gennes, *The Physics of Liquid Crystals* (Clarendon, Oxford, 1974).
[37] J. R. Kelly and P. Palffy-Muhoray (unpublished).
[38] P. G. Morse and H. Feshbach, *Methods of Theoretical Physics* (McGraw Hill, New York, 1953).
[39] H. Lin, P. Palffy-Muhoray, and M. A. Lee, Mol. Cryst. Liq. Cryst. **204**, 189 (1991).
[40] V. P. Romanov and A. N. Shalaginov, Zh. Eksp. Teor. Fiz. **102**, 884 (1992) [Sov. Phys. JETP **75**, 483 (1992)].
[41] F. Noack, M. Notter, and W. Weiss, Liq. Cryst. **3**, 907 (1988).
[42] G. P. Crawford, R. Stannarius, and J. W. Doane, Phys. Rev. A **44**, 2558 (1991).
[43] G. Iannacchione and D. Finotello, Liq. Cryst. **14**, 1135 (1993).
[44] J. Struppe, H. Gotzig, D. Schwarze-Haller, and F. Noack, *Abstracts of the 15th International Liquid Crystal Conference, Budapest, 1994* (Research Institute for Solid State Physics, Budapest, 1994), p. 486.
[45] J. Struppe, private communication.